



## โพรไฟล์ลิพิดมิกส์ในเซลล์ไฟбросบลัสต์ที่สัมพันธ์กับมะเร็งในผู้ป่วยมะเร็งท่อน้ำดี

นิษณา นามวاط<sup>\*1,2</sup>, ศรินทร์ญา ลิทธิรักษ์<sup>1,2</sup>, สายจิม ศรีจาน<sup>2,3</sup>, หญิงกัญญาภัชญ์ กิตติรัตน์<sup>4</sup>,  
อาภรณ์ หวังวิวัฒน์สิน<sup>1,2</sup>, ประเมษฐ์ กลั่นฤทธิ์<sup>1,2</sup>, อรรถพล ติตะปัญ<sup>2,5</sup>, วชิรินทร์ ลอยลม<sup>1,2</sup>

<sup>1</sup>โครงการจัดตั้งสาขาวิชาชีววิทยาศาสตร์ระบบและ การแพทย์เชิงคอมพิวเตอร์ คณะแพทยศาสตร์มหาวิทยาลัยขอนแก่น ขอนแก่น ประเทศไทย

<sup>2</sup>สถาบันวิจัยมะเร็งท่อน้ำดี มหาวิทยาลัยขอนแก่น ขอนแก่น ประเทศไทย

<sup>3</sup>สาขาวิชาชีวเคมี คณะแพทยศาสตร์ มหาวิทยาลัยขอนแก่น ขอนแก่น ประเทศไทย

<sup>4</sup>ศูนย์วิทยาศาสตร์การแพทย์ที่ 2 พิษณุโลก กรมวิทยาศาสตร์การแพทย์ พิษณุโลก ประเทศไทย

<sup>5</sup>ภาควิชาศัลยศาสตร์ คณะแพทยศาสตร์ มหาวิทยาลัยขอนแก่น ขอนแก่น ประเทศไทย

### Lipidomic Profiles of Cancer-Associated Fibroblasts with Cholangiocarcinoma Patients

Nisana Namwat<sup>1,2\*</sup>, Sirinya Sittirak<sup>1,2</sup>, Saikhim Sringan<sup>2,3</sup>, Yingpinyapat Kittirat<sup>4</sup>,  
Arporn Wangwiwatsin<sup>1,2</sup>, Poramate Klanrit<sup>1,2</sup>, Attapol Titapun<sup>1,5</sup>, Watcharin Loilome<sup>1,2</sup>

<sup>1</sup>Department of Systems Biosciences and Computational Medicine, Faculty of Medicine, Khon Kaen University, Khon Kaen, Thailand

<sup>2</sup>Cholangiocarcinoma Research Institute, Faculty of Medicine, Khon Kaen University, Khon Kaen, Thailand

<sup>3</sup>Medical Biochemistry and Molecular Biology Program, Department of Biochemistry, Faculty of Medicine, Khon Kaen University, Thailand

<sup>4</sup>Regional Medical Sciences Center 2 Phitsanulok, Department of Medical Sciences, Ministry of Public Health, Thailand

<sup>5</sup>Department of Surgery, Faculty of Medicine, Khon Kaen University, Khon Kaen, Thailand

Received: 25 December 2024/ Review: 28 December 2024/ Revised: 5 February 2025/

Accepted: 6 February 2025

\*Corresponding author: Nisana Namwat, E-mail: nisana@kku.ac.th

## บทคัดย่อ

**หลักการและวัตถุประสงค์:** ลิพิดเป็นองค์ประกอบสำคัญในมะเร็งโดยมีบทบาทในการส่งเสริมให้มะเร็งลุก窜และแพร่กระจาย เชลล์ cancer-associated fibroblasts (CAFs) ถือเป็นเซลล์ที่สำคัญอยู่ในสภาพแวดล้อมของมะเร็ง (tumor microenvironment; TME) ที่สร้างลิพิดแล้วส่งให้เซลล์มะเร็งนำไปใช้งาน วัตถุประสงค์ของการศึกษานี้เพื่อตรวจวิเคราะห์ชนิดของลิพิดใน CAFs ที่แยกสกัดจากเนื้อยื่มมะเร็งของผู้ป่วยมะเร็งท่อน้ำดีด้วยเทคนิคลิพิดมิกส์ซึ่งไม่เคยมีรายงานมาก่อน

**วิธีการศึกษา:** แยกสกัด CAFs จำนวน 3 ตัวอย่าง จากชิ้นเนื้อยื่มมะเร็งท่อน้ำดีและเพาะเลี้ยงในห้องทดลองให้เป็นเซลล์เพาะเลี้ยงปฐมภูมิ และตรวจวิเคราะห์โดยไฟล์ลิพิดมิกส์ในเซลล์ CAFs เปรียบเทียบกับเซลล์เพาะเลี้ยงไฟบอร์บลัสต์ปกติ (Normal fibroblasts; NF) ด้วยเทคนิคอัลตราไบโอร์ฟอร์แมนซ์ลิคิวิดโครมาโทกราฟี-แทนเดมแมสสเปกโทรมetri (UHPLC-MS/MS) และกระบวนการทางสกัตติ

**ผลการศึกษา:** การวิเคราะห์ชนิดลิพิดด้วย UHPLC-MS/MS ใน CAFs พบริพิดทั้งหมดจำนวน 43 ชนิด ใน 3 กลุ่ม ได้แก่ phosphatidylethanolamines, sphingomyelins และ phosphatidylcholines โดยมีปริมาณที่แตกต่างกันระหว่าง CAFs ที่แยกได้จากผู้ป่วย และ NFs อย่างมีนัยสำคัญทางสถิติ ( $p < 0.05$ )

**สรุป:** ชนิดของลิพิดที่พบใน CAFs ทั้ง 3 ชนิดนี้มีปริมาณแตกต่างกันและแตกต่างจาก NF และลิพิดชนิดที่พบนี้เกี่ยวข้องกับ metabolic adaptation ในการส่งเสริมกระบวนการเจริญเติบโตและการลุก窜ของมะเร็งท่อน้ำดี โดยไฟล์ลิพิดใน CAFs นี้ มีศักยภาพที่จะนำไปประยุกต์ใช้ในการรักษาแบบมุ่งเป้าที่ขัดขวางปฏิกิริยานิวเคลียร์และตับอลิซิเมะระหว่าง CAFs และ เชลล์มะเร็งท่อน้ำดี

**คำสำคัญ:** เซลล์ไฟบอร์บลัสต์ที่สัมผัสถกับมะเร็ง, มะเร็งท่อน้ำดี, เทคนิคลิพิดมิกส์

## Abstract

**Background and Objectives:** Lipids is an essential component in tumor and they facilitate tumor growth and metastasis. Cancer-associated fibroblasts (CAFs) are defined as a tumor environment (TME) by which cells reside in stromal compartments supporting tumor progression. The lipid profile of CAFs, particularly in cholangiocarcinoma (CCA), have been unexploited. We aimed to investigate lipid profiles in CAFs of patients with CCA using lipidomic approach.

**Methods:** Three samples of CAFs were primarily isolated from tumor tissues of patients with CCA and subcultured in the laboratory. Lipid profiles in CAFs compared with normal fibroblasts (NFs) were analyzed by a non-targeted lipidomic analysis platform using ultra-high performance liquid chromatography-tandem mass spectroscopy (UHPLC-MS/MS).

**Results:** Forty-three lipid species in 3 groups were determined in CAFs including phosphatidylethanolamines, sphingomyelins and phosphatidylcholines. Those lipids presented in different levels between CAFs and NFs.

**Conclusion:** Lipids in CAFs are associated with metabolic adaptation that might support tumor progression and metastasis in CCA. The lipid profiles in these CAFs have the potential to be applied in targeted therapies that disrupt metabolic interactions between CAFs and CCA cells.

**Keywords:** cancer-associated fibroblasts, cholangiocarcinoma, lipidomics.

## Introduction

Cholangiocarcinoma (CCA), a malignant tumor of bile duct epithelial lining, is one of the most common cancers and a significant public health problem in the Northeast Thailand<sup>1</sup>. Its development is strongly associated with Opisthorchiasis leading to chronic inflammation, which results in a dense, fibrous stroma marked by an aberrant growth of cancer-associated fibroblasts (CAFs)<sup>2</sup>. Markers of CAF activation in the stroma of patients with CCA consistently correlate with lymph node metastasis and reduced overall survival<sup>3</sup>. CAFs have been shown to actively contribute to cancer progression across various cancer types<sup>4-8</sup>. CAFs affect the behavior of epithelial cancer cells by releasing a range of metabolites and soluble factors that impact the metabolism, transcriptome, and signaling pathways in cancer cells<sup>9-11</sup>. Lipids are crucial energy sources and act as signaling molecules inside and outside cells. They support cell membrane integrity, provide essential nutrients, play a role in forming small extracellular vesicles<sup>12</sup>, and act as key second messengers in signal transduction<sup>13</sup>. This adaptation is essential for their growth, proliferation, and tumor metastasis<sup>14</sup>. Lipidomics reveals that CAF-derived lipids promote colorectal cancer peritoneal metastasis by enhancing membrane fluidity<sup>14</sup>. In this study, we aimed to investigate lipid profiles in CAFs of patients with CCA using lipidomic approach to gain a better understanding of the tumor microenvironment in CCA, clarify how lipid metabolism in CAFs contributes to CCA progression, and identify new lipid biomarkers for diagnosis or prognosis. This approach also applies to targeted therapies that disrupt metabolic interactions in CCA.

## Materials and Methods

### Patients, Samples, and Ethical issues

CAF Samples (J132, K088, and K112) were obtained from CCA tissues of patients who had surgical resection at Srinagarind Hospital. All patients provided written informed consent following the

guidelines of the Declaration of Helsinki and its subsequent amendments. The study protocol received approval from the Human Research Ethics Committee at Khon Kaen University (approval numbers #HE571283 and #HE611544). Primary human dermal fibroblasts (defined as normal fibroblasts; NFs), catalogue number ATCC® PCS-201-012™, were purchased from the American Type Culture Collection (ATCC) (Virginia, US).

### Reagents

Solvents including methanol, acetone, chloroform, and water of high-performance liquid chromatography (HPLC) quality were acquired from Merck (Darmstadt, DE). Dulbecco's Modified Eagle Medium (DMEM), heat-inactivated FBS were purchased from Thermo Fisher Scientific (California, USA). Glutamine and Penicillin/Streptomycin were obtained from Sigma-Aldrich (St. Louis, MO, USA). Rabbit polyclonal anti- $\alpha$ -SMA and anti-cytokeratin-19 antibodies were purchased from Abcam (Cambridge, UK).

### Primary Isolation of CAFs and Culturing

Tissues collected from 3 patients with diagnosed CCA, which underwent surgical resection at Srinagarind Hospital, Khon Kaen University, were in part of fibrosis close to tumor or adjacent areas. Fresh tissues of each patient were preserved in Hank's Balanced Salt Solution (HBSS) with antibiotics. Tissues were finely chopped into small pieces and digested by type IV collagenase at 37°C for 30 min. Once the enzymatic reaction had stopped, the tube was centrifuged at 2,000 rpm for 5 min to collect cell pellets. Cell precipitate was suspended with DMEM supplemented with 10% FBS and 100 IU/ml of penicillin-streptomycin. The suspended cells were filtrated through the cell strainer. The separated cells and retained pieces of tissues were cultured in each flask containing culture medium, at 37°C in a humidified atmosphere containing 5% CO<sub>2</sub>. Cultured cells were observed periodically, and epithelial cells were

aseptically scraped off. Fibroblasts were then transferred to new flasks and cultured until reaching confluence. Fibroblast cells were collected for cryofrozen cells with FBS contained filtrated 10% dimethyl sulfoxide. After subculturing for 2 - 3 passages (14 days) to acclimatize with their environment, CAFs were identified as a cell positive with  $\alpha$ -smooth muscle actin ( $\alpha$ -SMA) but negative with cytokeratin-19 using an immunofluorescence staining as described previously<sup>15</sup>.

#### Sample Collection and Preparation for LC-MS Lipid Profiling

CAF (Subpassage No. 3, 14-day subculture) and NF cells ( $2 \times 10^6$  cells) were collected by detaching them from dish using trypsin-EDTA and then centrifuged at 2,000 rpm at 4°C for 5 min. The cell pellets were washed with PBS for 3 times to remove the remaining medium and immediately frozen with liquid nitrogen. For lipid extraction, the frozen cells were resuspended in methanol and sonicated at 40% amplitude for 3 cycles. The lysed cells were phase- extracted using water/methanol/chloroform (1:1:3 v/v), incubated on ice for 20 min and centrifuged at 4,000 rpm at 4°C for 20 min. The organic phase was collected and transferred to a glass vial tube (KIMA, Arzegrande, IT), followed by drying the solvent under a fume hood overnight. The dried lipid extracts were reconstituted in a 200  $\mu$ L solvent mixture of isopropanol/acetonitrile/ $H_2O$  (2:1:1 v/v), and centrifuged for 20 min at 13,000 xg, 4°C. For each sample, 20  $\mu$ L was collected, pooled, and then used as a quality control (QC) sample for each interval throughout the analysis.

#### UHPLC-QTOF-MS Based Lipidomics

Lipidomics was carried out using ultra-high performance liquid chromatography coupled with electrospray ionization-quadrupole time-of-flight mass spectrometry (compact UHPLC ESI-Q-TOF MS, Bruker, DE). The lipid extracts were analyzed on a reverse-phase UHPLC system as previously described<sup>16</sup>.

#### Data Processing and Lipid Identification

The data were processed using MetaboScape software 5.0 (Bruker, Massachusetts, US) and converted to .csv files. Lipid identification was performed by comparing the MS/MS fragmentation patterns of detected features against public databases, using MS-DIAL software version 4.2 (RIKEN Center for Sustainable Resource Science, Kanagawa, JP), the Human Metabolome Database (HMDB), the Bruker Metabobase, and the LipidBlast database. The levels of assignment (LoA) included: (1) accurate mass matching to the database indicating a tentative assignment, (2) accurate mass and tandem MS spectrum matching to an in-silico fragmentation pattern, (3) tandem MS spectrum matching to the database or literature, (4) retention time and molecular mass matching to a standard compound, and (5) MS/MS spectrum matching to a standard compound<sup>16</sup>.

#### Statistical Analysis

Principal Component Analysis (PCA) was performed for data modeling and statistical analysis, along with the generation of heatmaps using MetaboAnalyst 6.0 (<https://www.metaboanalyst.ca/>). The heatmap illustrated the overall patterns of lipid composition across different samples, with hierarchical clustering revealing similar expression profiles. Python software version 3.10.12 was used to generate box plots. Differences in lipid compositions between samples were assessed using ANOVA, and a p-value of less than 0.05 was considered statistically significant.

## Results

#### Isolation and Characterization of Cancer-Associated Fibroblasts

We isolated CAFs from 3 CCA patients' tissues. Since the isolated CAFs presented a spindle-like morphology, we performed immunofluorescence to stain the expression of a CAF marker ( $\alpha$ -SMA). CK-19, an epithelial cell marker, was used to confirm non-contamination with epithelial cells. The results showed that all isolated CAFs expressed  $\alpha$ -SMA (Fig. 1).

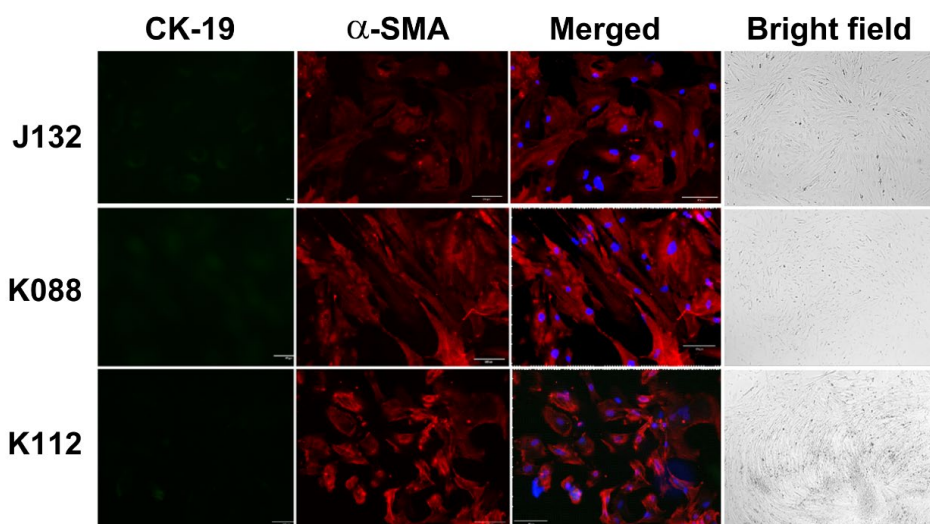


**Fig. 1** Characterization of CAFs by immunofluorescence staining. CAFs displayed a spindle-like morphology by  $\alpha$ -SMA staining observed under a fluorescence microscope. DAPI staining (blue color) was used for visualizing the nuclei of CAFs. Green, stained with cytokeratin-19 (CK-19); red, stained with  $\alpha$ -SMA. The original magnification is  $\times 100$ . A bright-field microscopic images of CAFs were magnified at  $\times 10$ .

#### Metabolic Distinctions and Subtype-specific Adaptations in CAFs Revealed by PCA and PLS-DA

The identification of lipid candidates in primary isolated-CAFs was shown in Table 1. Principal Component Analysis (PCA) and Partial Least Squares Discriminant Analysis (PLS-DA) were conducted to assess the metabolites' differences between cancer-associated fibroblasts (CAFs) and normal fibroblasts (NFs). The PCA score plot demonstrated a distinct separation between the CAFs (CAF-J132, CAF-K088, CAF-K112) and NFs, signifying unique overall metabolic profiles (Fig. 2A-B). The initial two principal components explained a substantial fraction of the variance in the data, underscoring the metabolic heterogeneity of CAF subtypes while preserving clear distinctions from NFs.

The PLS-DA score plot further elucidated these findings, highlighting the selective capability of particular metabolites in differentiating CAFs from NFs (Fig. 2C-D). CAF subtypes demonstrated metabolic clustering, with CAF-K088 displaying unique traits in contrast to CAF-J132 and CAF-K112, indicating subtype-specific metabolic adaptations.

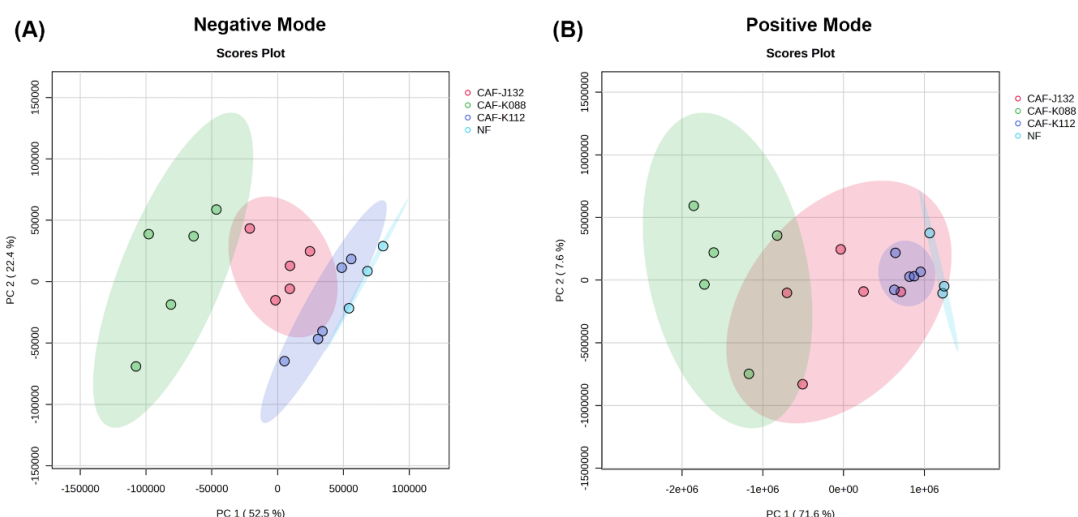
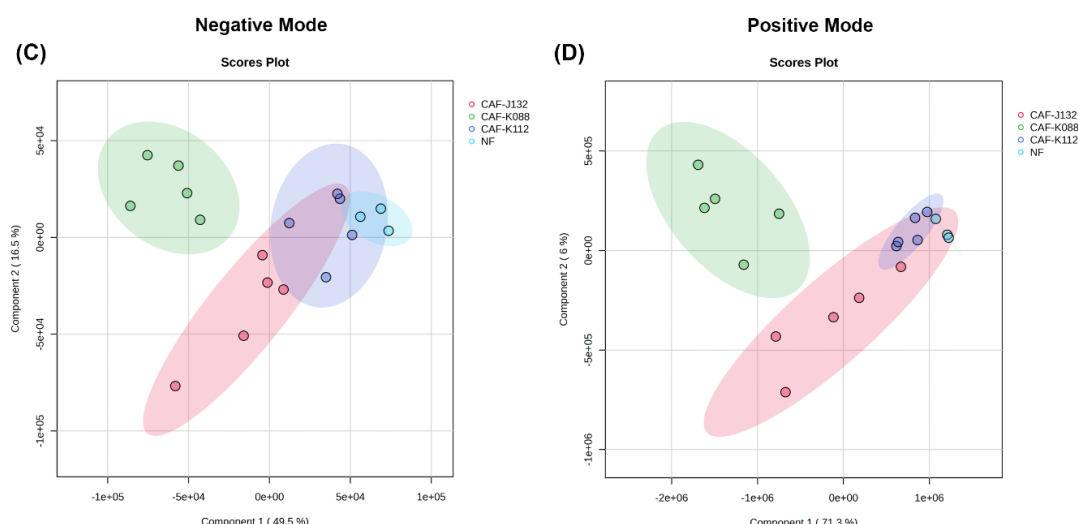
The loading plots from PLS-DA highlighted metabolites with elevated variable importance in projection (VIP) scores, emphasizing their significance in facilitating group distinction. We selected  $\text{VIP} \geq 1.0$  and  $\text{ANOVA P-value} < 0.05$  as the standard cut-off for identifying important metabolites. These findings underscore substantial metabolic reprogramming in CAFs relative to NFs and disclose subtype-specific metabolic variability within CAFs. The identified patterns indicate a functional metabolic alteration in CAFs that may enhance their pro-tumorigenic functions within the tumor microenvironment.

**Table 1** The identification of lipid candidates in primary isolated-CAFs.

Metabolites	Formula	Adduct	RT	m/z	VIP score
PE 34:1	C39H76NO8P	[M+H]-	10.93	716.52407	2.9232
PE 36:2	C41H78NO8P	[M+H]-	10.98	742.53981	0.40389
PE 36:5e	C41H74NO7P	[M+H]-	9.36	722.51342	0.87048
PE 38:4	C43H78NO8P	[M+H]-	10.97	766.53991	0.0034357
PE 38:5	C43H76NO8P	[M+H]-	8.35	764.52433	0.70109
PE 38:5e	C43H78NO7P	[M+H]-	12.34	750.54529	0.073886
1-Stearoyl-2-Arachidonoyl PC	C46H84NO8P	[M+H]+	12.11	810.60171	1.5128
Eicosapentaenoyl PAF C-16	C44H80NO7P	[M+H]+	10.27	766.57476	0.098562
PC 30:0	C38H76NO8P	[M+H]+	9.23	706.53817	1.1421
PC 30:1	C38H74NO8P	[M+H]+	7.12	704.5216	2.216
PC 31:0	C39H78NO8P	[M+H]+	10.63	720.55363	13.107
PC 31:1	C39H76NO8P	[M+H]+	8.15	718.53703	0.98219
PC 32:1	C40H78NO8P	[M+H]+	9.39	732.55399	2.5026
PC 32:2	C40H76NO8P	[M+H]+	7.41	730.5379	0.063276
PC 33:1	C41H80NO8P	[M+H]+	10.66	746.56971	0.091936
PC 34:0	C42H84NO8P	[M+H]+	14.2	762.60128	1.4967
PC 34:1	C42H82NO8P	[M+H]+	12.19	760.58547	0.32292
PC 34:1e	C42H84NO7P	[M+H]+	13.74	746.60642	9.1043
PC 34:2	C42H80NO8P	[M+H]+	9.82	758.56983	0.99887
PC 34:3	C42H78NO8P	[M+H]+	7.55	756.55392	3.1036
PC 34:4	C42H76NO8P	[M+H]+	9.45	754.53651	1.1668
PC 35:1	C43H84NO8P	[M+H]+	13.49	774.60127	0.085365
PC 35:2	C43H82NO8P	[M+H]+	10.69	772.58513	1.871
PC 36:1	C44H86NO8P	[M+H]+	14.16	788.6172	0.14163
PC 36:3	C44H82NO8P	[M+H]+	9.82	784.58586	0.36881
PC 36:4	C44H80NO8P	[M+H]+	9.15	782.56991	0.29411
PC 36:5	C44H78NO8P	[M+H]+	7.64	780.55397	0.040635
PC 37:5	C45H80NO8P	[M+H]+	8.03	794.56991	2.8934
PC 38:5	C46H82NO8P	[M+H]+	9.18	808.58582	2.9561
PC 38:6	C46H80NO8P	[M+H]+	8.46	806.56988	0.34017
PC 40:5	C48H86NO8P	[M+H]+	12.27	836.61711	0.32169
PC 40:6	C48H84NO8P	[M+H]+	9.27	834.60201	1.6284
PC 40:7	C48H82NO8P	[M+H]+	8.43	832.58586	1.8396
PC_16:00_16:00	C40H80NO8P	[M+H]+	12.2	734.56967	1.1053
PC_18:01_9Z_18:01_9Z	C44H84NO8P	[M+H]+	12.17	786.60151	0.62906
PE 38:4	C43H78NO8P	[M+H]+	10.94	768.55576	0.93759
PS 36:1	C42H80NO10P	[M+H]+	10.88	790.55585	0.34254
SM d34:0	C39H81N2O6P	[M+H]+	9.95	705.59022	0.81973

**Table 1** The identification of lipid candidates in primary isolated-CAFs. (Cont.)

Metabolites	Formula	Adduct	RT	m/z	VIP score
SM d34:1	C39H79N2O6P	[M+H]+	8.95	703.57487	4.964
SM d34:2	C39H77N2O6P	[M+H]+	6.97	701.5593	0.41803
SM d40:1	C45H91N2O6P	[M+H]+	15.44	787.6686	0.79457
SM d42:1	C47H95N2O6P	[M+H]+	16.92	815.70144	0.32991
SM d42:2	C47H93N2O6P	[M+H]+	15.2	813.68572	0.75798

**Principle Component Analysis (PCA)****Partial Least Squares Discriminant Analysis (PLS-DA)**

**Fig. 2** Summary of metabolic profiling of Cancer-Associated Fibroblasts (CAFs) and Normal Fibroblasts (NFs). PCA (A, B) and PLS-DA (C, D) analyses in negative and positive modes, respectively, reveal distinct metabolic profiles between CAFs (CAF-J132, CAF-K088, and CAF-K112) and NFs. Clustering patterns indicate metabolic heterogeneity among CAF subtypes, with CAF-K088 showing unique features.

## Lipid Metabolic Alterations in CAFs: A Comparative Analysis with NFs

The heatmap analysis demonstrated notable disparities in the metabolic profiles of CAFs relative to NFs. Hierarchical clustering clearly differentiated the three CAF lines (CAF-J132, CAF-K088, and CAF-K112) from the NFs, emphasizing differential lipid/metabolite expression profiles in CAFs. Numerous metabolites were significantly elevated in CAFs, including phosphatidylcholines (PC 34:3, PC 38:6, and PC 36:4), phosphatidylethanolamines (PE 36:2 and PE 38:4), and sphingomyelins (SM d42:2 and SM d42:1). The findings indicate an enhancement in membrane lipid production and sphingolipid metabolism, essential for cellular signaling and structural integrity within the tumor microenvironment. PC 34:3 exhibited notably elevated expression in CAF-K088, indicating subtype-

specific metabolic activity. In contrast, metabolites including eicosapentaenoyl phosphatidylcholine and PE 40:5 were downregulated in CAFs relative to NFs, suggesting a possible inhibition of lipid species associated with anti-inflammatory or oxidative stress pathways. Significantly, SM d42:2 was consistently raised in all CAF subtypes, indicating a common metabolic adaption to facilitate the pro-tumorigenic functions of CAFs. The metabolic disparities between CAFs and NFs suggest a transition in lipid metabolism, presumably influenced by the requirements of the tumor microenvironment. These findings offer significant insights into the metabolic reprogramming of CAFs, which may affect their interactions with tumor cells and identify prospective targets for therapeutic intervention.

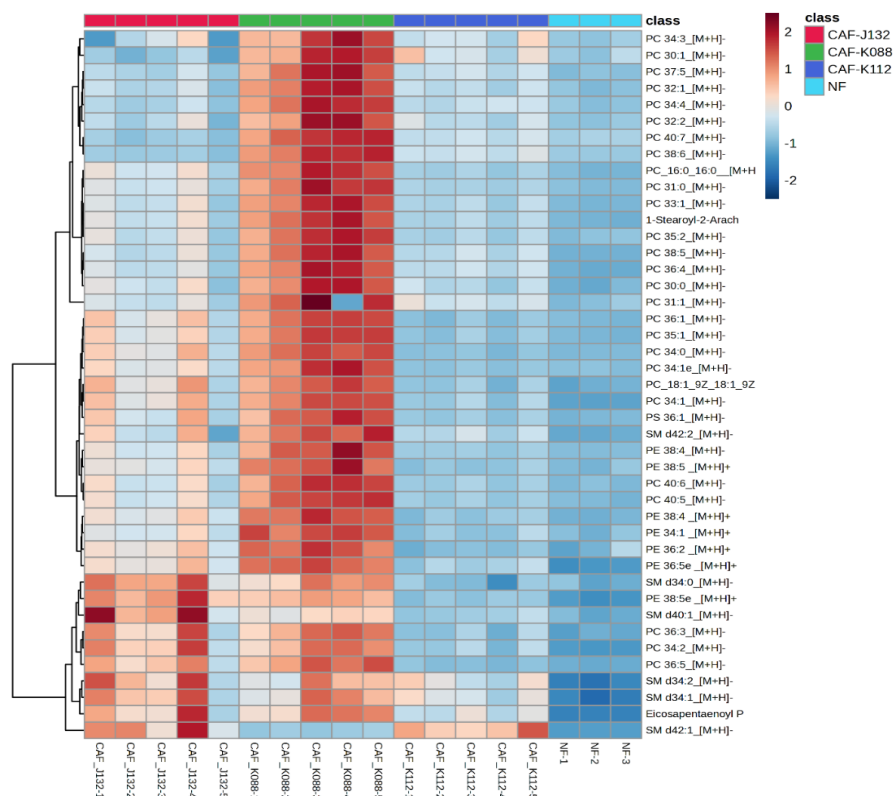


**Fig. 3** Heatmap depicting the varying metabolite expression profiles of CAFs compared to NFs. The CAF groups (CAF-J132, CAF-K088, and CAF-K112) and the NF group are categorized by hierarchical analysis. Rows denote distinct lipid/metabolite species, encompassing phosphatidylcholines (e.g., PC 34:3, PC 38:6, PC 36:4), phosphatidylethanolamines (e.g., PE 36:2, PE 38:4), and sphingomyelins (e.g., SM d42:2, SM d42:1). Columns represent distinct samples from each group. The color gradient represents normalized intensity levels, where red signifies elevated expression and blue denotes diminished expression. Clustering patterns indicate substantial metabolic reprogramming in CAFs versus NFs, characterized by increased concentrations of critical lipids like PC 34:3, SM d42:2, and PE 38:4 in CAFs, and diminished levels of metabolites such as eicosapentaenoyl phosphatidylcholine in CAFs compared to NFs.

## Metabolic Reprogramming in CAFs: Evidence from Key Metabolite Comparisons

Box plot analysis was employed to evaluate the expression levels of critical metabolites between CAFs and NFs. The findings underscore substantial variations in metabolite concentrations, reinforcing the concept of metabolic reprogramming in CAFs. Metabolites including phosphatidylcholines (PC 34:3 and PC 38:6), phosphatidylethanolamines (PE 36:2 and PE 38:4), and sphingomyelins (SM d42:2) showed significantly elevated levels in CAFs relative to NFs ( $p < 0.05$ ). The higher levels are consistent among CAF subtypes (CAF-J132, CAF-K088, and CAF-K112), with CAF-K088 exhibiting the most significant variations for specific metabolites, including PC 34:3.

In contrast, metabolites such eicosapentaenoyl phosphatidylcholine and PE 40:5 exhibited markedly reduced levels in CAFs compared to NFs, suggesting a targeted inhibition of particular metabolic pathways in CAFs. The interquartile range (IQR) illustrated in the box plots further exemplifies the metabolic variety among CAF subtypes, indicating that these cells modify their metabolic profiles according to their functional roles within the tumor microenvironment.

These results corroborate the metabolic alterations identified in CAFs and underscore potential indicators for differentiating CAFs from normal fibroblasts. The persistent increase of certain metabolites in all CAFs highlights their possible involvement in facilitating tumor advancement.

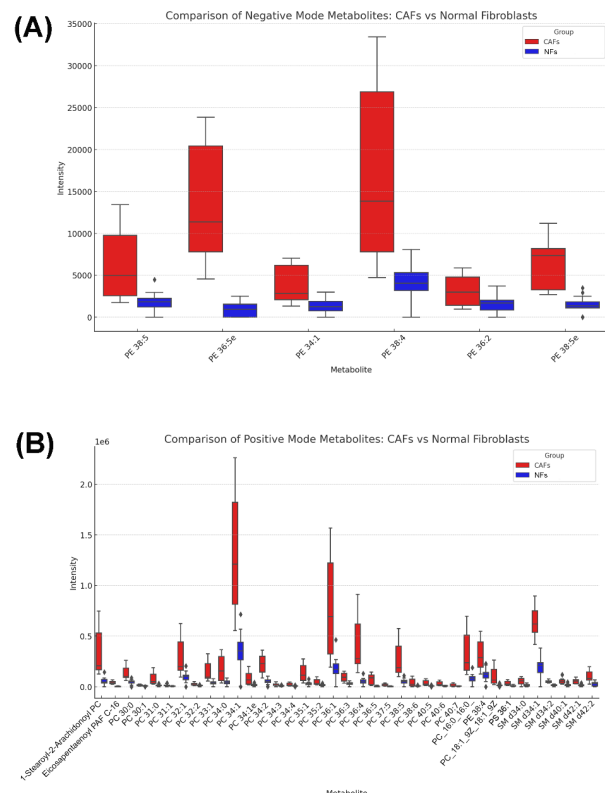


**Fig. 4** Box plots showing differential metabolite expression between CAFs and NFs. Variability among CAF subtypes reflects metabolic heterogeneity. Statistical significance ( $p < 0.05$ ) highlights key differences, emphasizing metabolic reprogramming in CAFs. (A) Negative mode. (B) Positive mode.

## Discussion

Our study provides an in-depth exploration of the lipidomic profiles in CAFs, highlighting reprogrammed lipid metabolism as a distinctive feature of CAFs within the tumor environment. Lipid metabolism in CAFs may play a crucial role in tumor progression by fueling cancer cell metabolism, activating survival pathways, promoting metastasis, inducing drug resistance, and suppressing immune responses.<sup>4-8</sup> Through liquid chromatography-tandem mass spectrometry (LC-MS/MS) and principal component analysis (PCA), we established a distinct separation in lipid profiles between CAFs and NF cells. The uniqueness of lipid composition is emphasized across multiple analytical perspectives, providing a robust characterization of metabolic divergence.

The study identifies 43 lipid species that distinguish CAFs from NF cells, with notable increases in phosphatidylcholines, phosphatidylethanolamines, and sphingomyelins. This indicates a distinct metabolic shift in CAFs, reinforcing the view that tumor-associated fibroblasts undergo lipid reprogramming to support cancer progression. These findings reflect similar lipid metabolism observations in other cancer models, where CAFs adapt their lipidomic profiles to promote cell survival and proliferation in a nutrient-scarce tumor microenvironment<sup>14,17</sup>. Using LC-MS/MS to conduct a detailed lipidomic analysis, PCA was employed to map the differences, showing a clear separation between CAF and NF lipid profiles. This analytical approach aligns with studies that use LC-MS/MS to capture specific lipidomic patterns, which are valuable in distinguishing in various cell types<sup>18,19</sup>. Lipid types, such as phosphatidylcholines (PCs), phosphatidylethanolamines (PEs), and sphingomyelins (SMs), were more abundant in CAFs, suggesting their potential as biomarkers for tumor microenvironment characterization. These findings parallel similar research in oncology, where lipid biomarkers are utilized for diagnostic or prognostic insights<sup>20</sup>. The study's heatmap analysis reveal that plasma membrane-associated lipids, particularly phosphatidylethanolamines (PEs), were more prevalent in CAFs than in NF cells. Sphingomyelins, integral to membrane structure and cell signaling, appear elevated, hinting at their role in modified membrane behavior essential to CAFs' support functions within the tumor. This aspect is particularly interesting as it aligns with recent studies showing that sphingolipid metabolism contributes to tumor cell adaptation in hypoxic or nutrient-deprived microenvironments<sup>21</sup>. This observation suggests that CAFs not only adjust their lipid profiles for structural purposes but may also rely on these changes for vesicular trafficking, potentially facilitating the secretion of growth factors or exosomes that support CCA cells. Studies on other cancers have similarly noted the role of vesicular trafficking in cancer-associated fibroblast function,

suggesting a broader oncological mechanism<sup>22</sup>. CAFs are a diverse cell population, exhibiting significant heterogeneity. Different CAF subtypes can have distinct functions and behaviors within the tumor microenvironment. One key aspect of this heterogeneity is reflected in their lipidomic profiles. Nevertheless, the unique lipid profiles in CAFs suggest a potential for developing lipid-based biomarkers that could aid in distinguishing CAFs from cancer cells. As CAFs undergo significant lipid metabolic reprogramming in response to tumor signals, their lipidomic profile can indicate tumor presence, aggressiveness, and therapy resistance. Further investigation of lipid profiles in blood samples from CCA patients could help identify potential prognostic markers for monitoring disease progression and improving therapeutic outcomes.

## Conclusion

This approach could improve the precision of diagnostics in tumor microenvironment characterization, offering a non-invasive tool for distinguishing cellular components within tumors. This is consistent with evolving research directions in biomarker discovery, which aim to identify metabolic and lipidomic markers that provide insight into the tumor ecosystem and its cellular interactions<sup>23</sup>.

## Acknowledgements

This work was supported by a grant from Faculty of Medicine, Khon Kaen University (Grant no. IN64122) to S.S. and N.N.

## References

1. Sahat O, Kamsa-Ard S, Suwannatrat AT, Lim A, Kamsa-Ard S, Bilheem S, et al. Spatial analysis of cholangiocarcinoma in Thailand from 2012 to 2021; a population-based cancer registries study. PLoS One 2024;19(12):e0311035. doi:10.1371/journal.pone.0311035.
2. Sripa B, Brindley PJ, Mulvenna J, Laha T, Smout MJ, Mairiang E, et al. The tumorigenic liver fluke *Opisthorchis viverrini*--multiple pathways to cancer. Trends Parasitol 2012;28(10):395-407. doi: 10.1016/j.pt.2012.07.006.

3. Zhang XF, Dong M, Pan YH, Chen JN, Huang XQ, Jin Y, et al. Expression pattern of cancer-associated fibroblast and its clinical relevance in intrahepatic cholangiocarcinoma. *Hum Pathol* 2017;65:92-100. doi:10.1016/j.humpath.2017.04.014.
4. Comito G, Giannoni E, Segura CP, Barcellos-de-Souza P, Raspollini MR, Baroni G, et al. Cancer-associated fibroblasts and M2-polarized macrophages synergize during prostate carcinoma progression. *Oncogene* 2014;33(19):2423-31. doi:10.1038/onc.2013.191.
5. Hwang RF, Moore T, Arumugam T, Ramachandran V, Amos KD, Rivera A, et al. Cancer-associated stromal fibroblasts promote pancreatic tumor progression. *Cancer Res* 2008;68(3):918-26. doi:10.1158/0008-5472.CAN-07-5714.
6. Kramer N, Schmollerl J, Unger C, Nivarthi H, Rudisch A, Unterleuthner D, et al. Autocrine WNT2 signaling in fibroblasts promotes colorectal cancer progression. *Oncogene* 2017;36(39):5460-72. doi:10.1038/onc.2017.144.
7. Worzfeld T, Pogge von Strandmann E, Huber M, Adhikary T, Wagner U, Reinartz S, et al. The Unique Molecular and Cellular Microenvironment of Ovarian Cancer. *Front Oncol* 2017;7:24. doi:10.3389/fonc.2017.00024.
8. Raffaghelli L, Vacca A, Pistoia V, Ribatti D. Cancer associated fibroblasts in hematological malignancies. *Oncotarget* 2015;6(5):2589-603. doi:10.18632/oncotarget.2661.
9. Morandi A, Giannoni E, Chiarugi P. Nutrient Exploitation within the Tumor-Stroma Metabolic Crosstalk. *Trends Cancer* 2016;2(12):736-46. doi:10.1016/j.trecan.2016.11.001.
10. Chiarugi P, Cirri P. Metabolic exchanges within tumor microenvironment. *Cancer Lett* 2016;380(1):272-80. doi:10.1016/j.canlet.2015.10.027.
11. Kuzet SE, Gaggioli C. Fibroblast activation in cancer: when seed fertilizes soil. *Cell Tissue Res* 2016;365(3):607-19. doi:10.1007/s00441-016-2467-x.
12. Donoso-Quezada J, Ayala-Mar S, Gonzalez-Valdez J. The role of lipids in exosome biology and intercellular communication: Function, analytics and applications. *Traffic* 2021;22(7):204-20. doi:10.1111/tra.12803.
13. Zechner R, Zimmermann R, Eichmann TO, Kohlwein SD, Haemmerle G, Lass A, et al. FAT SIGNALS--lipases and lipolysis in lipid metabolism and signaling. *Cell Metab* 2012;15(3):279-91. doi:10.1016/j.cmet.2011.12.018.
14. Peng S, Li Y, Huang M, Tang G, Xie Y, Chen D, et al. Metabolomics reveals that CAF-derived lipids promote colorectal cancer peritoneal metastasis by enhancing membrane fluidity. *Int J Biol Sci* 2022;18(5):1912-32. doi:10.7150/ijbs.68484.
15. Kittirat Y, Suksawat M, Thongchot S, Padthaisong S, Phetcharaburanin J, Wangwiwatsin A, et al. Interleukin-6-derived cancer-associated fibroblasts activate STAT3 pathway contributing to gemcitabine resistance in cholangiocarcinoma. *Front Pharmacol* 2022;13:897368. doi:10.3389/fphar.2022.897368.
16. Kittirat Y, Phetcharaburanin J, Promraksa B, Kulthawatsiri T, Wangwiwatsin A, Klanrit P, et al. Lipidomic Analyses Uncover Apoptotic and Inhibitory Effects of Pyrvinium Pamoate on Cholangiocarcinoma Cells via Mitochondrial Membrane Potential Dysfunction. *Front Public Health* 2021;9:766455. doi:10.3389/fpubh.2021.766455.
17. Peng S, Chen D, Cai J, Yuan Z, Huang B, Li Y, et al. Enhancing cancer-associated fibroblast fatty acid catabolism within a metabolically challenging tumor microenvironment drives colon cancer peritoneal metastasis. *Mol Oncol* 2021;15(5):1391-411. doi:10.1002/1878-0261.12917.
18. Takanashi Y, Kahyo T, Sekihara K, Kawase A, Setou M, Funai K. Prognostic potential of lipid profiling in cancer patients: a systematic review of mass spectrometry-based studies. *Lipids Health Dis* 2024;23(1):154. doi:10.1186/s12944-024-02121-0.

19. Eiriksson FF, Nohr MK, Costa M, Bodvarsdottir SK, Ogmundsdottir HM, Thorsteinsdottir M. Lipidomic study of cell lines reveals differences between breast cancer subtypes. *PLoS One* 2020;15(4): e0231289. doi:10.1371/journal.pone.0231289.

20. Sah S, Bifarin OO, Moore SG, Gaul DA, Chung H, Kwon SY, et al. Serum Lipidome Profiling Reveals a Distinct Signature of Ovarian Cancer in Korean Women. *Cancer Epidemiol Biomarkers Prev* 2024; 33(5):681-93. doi:10.1158/1055-9965.EPI-23-1293.

21. Li RZ, Wang XR, Wang J, Xie C, Wang XX, Pan HD, et al. The key role of sphingolipid metabolism in cancer: New therapeutic targets, diagnostic and prognostic values, and anti-tumor immunotherapy resistance. *Front Oncol* 2022;12:941643. doi:10.3389/fonc.2022.941643.

22. Nedaeinia R, Najafgholian S, Salehi R, Goli M, Ranjbar M, Nickho H, et al. The role of cancer-associated fibroblasts and exosomal miRNAs-mediated intercellular communication in the tumor microenvironment and the biology of carcinogenesis: a systematic review. *Cell Death Discov* 2024;10(1):380. doi:10.1038/s41420-024-02146-5.

23. Jiang T, Dai L, Li P, Zhao J, Wang X, An L, et al. Lipid metabolism and identification of biomarkers in asthma by lipidomic analysis. *Biochim Biophys Acta Mol Cell Biol Lipids* 2021;1866(2):158853. doi:10.1016/j.bbalip.2020.158853.

